Article:
Greatorex, S, Vincent, KB, Baldansuren, A et al. (4 more authors) (2019) Rigidification of a macrocyclic tris-catecholate scaffold leads to electronic localisation of its mixed valent redox product. Chemical Communications, 55 (16). pp. 2281-2284. ISSN 1359-7345

https://doi.org/10.1039/C8CC10122A

Rigidification of a Macrocyclic *Tris*-Catecholate Scaffold Leads to Electronic Localisation of its Mixed Valent Redox Product

Sam Greatorex[a], Kevin B. Vincent[b], Amgalanbaatar Baldansuren[c], Eric J. L. McInnes[c], Nathan J. Patmore[b], Stephen Sproules[d] and Malcolm A. Halcrow[a,*]

The catecholate groups in [{Pt(L)}$_3$(μ_3-tctq)] (H_6tctq = 2,3,6,7,10,11-hexahydroxy-4b,8b,12b,12d-tetramethyltribenzotriquinacene; L = a diphosphine chelate) undergo sequential oxidation to their semiquinonate forms by voltammetry, with $\Delta E_{½}$ = 160–170 mV. The monoradical [{Pt(dppb)}$_3$(μ_3-tctq$^{\bullet}$)]$^+$ is valence-localised, with no evidence for intervalence charge transfer in its near-IR spectrum. This contrasts with previously reported [{Pt(dppb)}$_3$(μ_3-ctc$^{\bullet}$)]$^+$ (H_6ctc = cyclotricatechylene), based on the same macrocyclic *tris*-dioxolene scaffold, which exhibits partly delocalised (class II) mixed valency.

Dioxolenes are one of the most versatile and important non-innocent ligands for transition ions.[1] The catecholate (cat)/semiquinonate (sq) redox process occurs at low potential in metal-bound dioxolenes, which can lead to stable ligand radical species and/or facile charge transfer processes between the dioxolene and coordinated metal ion. This makes catecholate ligands useful electron reservoirs for catalysis[2,3] and biological redox reactions.[3,4] Alternatively, metal-bound sq radicals can act as switchable molecular paramagnets,[5] or show bulk magnetic ordering when incorporated into coordination frameworks.[6] Lastly, complexes containing multiple dioxolene centres can exhibit ligand-based mixed-valency[7] with intense inter-valence charge-transfer absorptions in the near-IR. This has been observed in both mononuclear [M(cat)$_3$] complexes,[8] and in complexes of more complicated organic scaffolds containing two or three linked dioxolene redox sites.[9-11]

In the latter vein, we recently re-investigated the complexes [{Pt(L)}$_3$(μ_3-ctc)] (H_6ctc = cyclotricatechylene; L = 1,2-*bis*{diphenylphosphinobenzene [dppb] or 1,2-*bis*{diphenylphosphinoethane [dppe]; Scheme 1), which were originally synthesised by Bohle and Stasko.[12] The three catecholate groups in these complexes are oxidised sequentially, leading to [{Pt(L)}$_3$(μ_3-ctc$^{\bullet}$)]$^+$ and [{Pt(L)}$_3$(μ_3-ctc$^{\bullet\bullet}$)]$^{2+}$ radical products showing class II mixed valency by UV/vis/NIR spectroscopy,[13] despite the absence of direct conjugation between their dioxolene redox centers.[14] The radical products of this work were too unstable to isolate however, and could only be handled in solution below room temperature. We reasoned this might reflect a lack of steric protection about the methylene groups of the oxidised [ctc]$^{n-}$ macrocycle, since sq and other phenoxyl radicals are prone to atom abstraction or coupling reactions at such *para* substituents.[15]

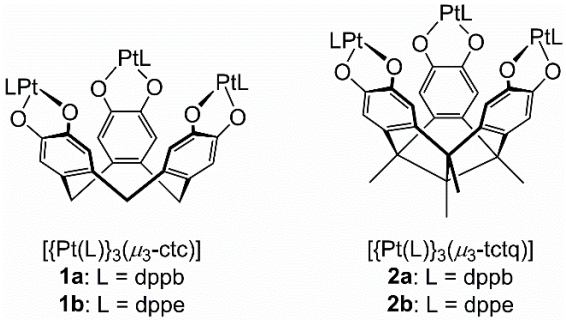

[{Pt(L)}$_3$(μ_3-ctc)]
1a: L = dppb
1b: L = dppe

[{Pt(L)}$_3$(μ_3-tctq)]
2a: L = dppb
2b: L = dppe

Scheme 1. The compounds described in this work.

Hence, we turned to the related tricatechol 2,3,6,7,10,11-hexahydroxy-4b,8b,12b,12d-tetramethyltribenzotriquinacene (H_6tctq; Scheme 1), which is a new variant of the rigid tribenzotriquinacene motif developed by Kuck[16] as a bowl-shaped scaffold for supramolecular architectures[17,18] and soft materials ¶.[19] Since the methylene groups linking the catechol rings in [tctq]$^{6-}$ are fully quaternised, we reasoned that radicals

[a] *School of Chemistry, University of Leeds, Woodhouse Lane, Leeds LS2 9JT, UK. Email: m.a.halcrow@leeds.ac.uk*
[b] *Department of Chemical Sciences, University of Huddersfield, Huddersfield HD1 3DH, UK.*
[c] *School of Chemistry and Photon Science Institute, University of Manchester, Oxford Road, Manchester M13 9PL, UK.*
[d] *WestCHEM, School of Chemistry, University of Glasgow, Glasgow G12 8QQ, UK.*

† Electronic Supplementary Information (ESI) available: Experimental procedures for the synthesis and physical and computational characterisation of the compounds in this work; crystallographic Figures and tables; EPR spectra and simulated parameters; and computed structures, MO manifolds, orbital and spin density plots. CCDC 1885699. For ESI and crystallographic data in CIF or other electronic format see DOI: 10.1039/######.

‡ Data supporting this study are available at http://doi.org/10.5518/###.

derived by oxidation of [{Pt(L)}$_3$(μ_3-tctq)] might be more stable and easier to isolate. In the event that was not observed, but we report here that sq radicals derived from [{Pt(L)}$_3$(μ_3-ctc)] (**1a**/**1b,** Scheme 1) and [{Pt(dppb)}$_3$(μ_3-tctq)] (**2a**) display unexpectedly different electronic properties.

2,3,6,7,10,11-Hexamethoxy-4b,8b,12b,12d-tetramethyltribenzotriquinacene is accessible in nine synthetic steps by a literature procedure (ESI†).[20] H_6tctq was obtained by exhaustive demethylation of this precursor using BBr_3 ¶. Compounds **2a** and **2b** were prepared by treatment of H_6tctq with 3 equiv of the appropriate [$PtCl_2$(L)] reagent in a *N*,*N*-dimethylacetamide/methanol solvent mixture, using potassium *tert*-butoxide as a base. While **2a** is soluble in weakly interacting solvents and stable under an inert atmosphere, **2b** is much less soluble and apparently less stable, so more limited characterisation of that compound was achieved. Similar issues were also encountered with **1b**.[14]

Differential pulse voltammograms of **2a** and **2b** in CH_2Cl_2/0.1M NBu_4PF_6 resemble those of **1a** and **1b**, in showing three closely spaced low-potential oxidations (Fig. 1).[14] These are assigned to sequential oxidation of the three cat rings in the [tctq]$^{6-}$ ligand to the sq oxidation level (eq 1).

$$[tctq]^{6-} \rightleftharpoons [tctq^{\bullet}]^{5-} \rightleftharpoons [tctq^{\bullet\bullet}]^{4-} \rightleftharpoons [tctq^{\bullet\bullet\bullet}]^{3-} \quad (1)$$

The first two processes for both compounds are chemically reversible and occur at similar potentials, but with $E_{½}$ *ca.* 50 mV more positive for **2b** than **2a** (Table 1). Some differences are seen on the third oxidation wave, however. The **[2a$^{\bullet\bullet}$]$^{2+}$/[2a$^{\bullet\bullet\bullet}$]$^{3+}$** oxidation is obviously split into two or three components implying some decomposition or deposition of the **[2a$^{\bullet\bullet}$]$^{2+}$** redox product. In contrast the **[2b$^{\bullet\bullet}$]$^{2+}$/[2b$^{\bullet\bullet\bullet}$]$^{3+}$** oxidation occurs at *ca.* 0.2 V higher potential, and is apparently clean. The separation between the first two oxidation potentials in **2a** and **2b**, $\Delta E_{½}$ = 0.16–0.17 V, yields the comproportionation constants K_c = 6-8 × 10^2 between each oxidation level.[10,13] That is slightly smaller than for **1a** and **1b** ($\Delta E_{½}$ = 0.18–0.22 V, K_c = 1–5 × 10^3),[14] which implies electronic communication between the dioxolene rings in coordinated [tctq]$^{n-}$ is weaker than for [ctc]$^{n-}$. A second series of irreversible processes at +0.75–1.2 V was observed for **2a**, assignable to further oxidation of the dioxolene rings in [tctq$^{\bullet\bullet\bullet}$]$^{3-}$ to the quinone level. These were less well-defined in **2b**, which might reflect its precipitation at the electrode during the measurement.

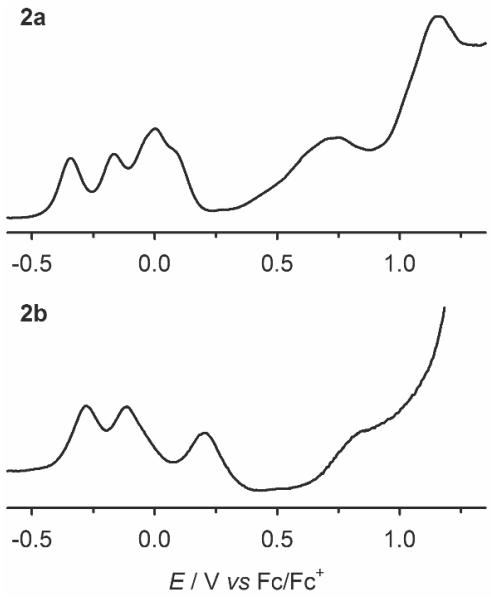

Fig. 1 Differential pulse voltammogram of **2a** and **2b** (CH_2Cl_2/0.1M NBu_4PF_6, 293 K).

Table 1 Electrochemical data for the complexes in this work (cat = catecholate; sq = semiquinonate; q = quinone). Potentials are referenced against $Fc^{+/0}$.

	sq/cat ($E_{½}$ / V)			q/sq (irr[a], Ep_a / V)
2a	–0.34	–0.17	+0.00, 0.08	+0.75, +1.16
2b	–0.28	–0.12	+0.20	+0.82

[a]irr = irreversible.

EPR spectra of **[2a$^{\bullet}$]$^{+}$** and **[2b$^{\bullet}$]$^{+}$**, generated by *in situ* oxidation of the neutral precursors with 1 equiv [Cp_2Fe]PF_6, were measured in frozen CH_2Cl_2 solution at X- and S-band frequencies. The spectra resemble **[1a$^{\bullet}$]$^{+}$** and other Pt(II)/sq radicals in showing weakly rhombic *g*-patterns, with hyperfine coupling to just one ^{195}Pt nucleus (ESI†).[14,21,22] That shows the unpaired electrons in **[2a$^{\bullet}$]$^{+}$** and **[2b$^{\bullet}$]$^{+}$** are localised on one dioxolene ring under these conditions, on the EPR timescale. Fluid solution EPR spectra in the same solvent were achieved for **[2a$^{\bullet}$]$^{+}$**, yielding simulated isotropic $A\{^{195}Pt\}$ and $a\{^{31}P\}$ values that are 30-50 % larger than for **[1a$^{\bullet}$]$^{+}$**. That is consistent with a greater degree of localisation of the unpaired spin in **[2a$^{\bullet}$]$^{+}$**.

The UV/vis spectra of **2a** and **2b** in CH_2Cl_2/0.1 M NBu_4PF_6 show just one resolved maximum at 31.7 × 10^3 cm^{-1}. Spectroelectrochemical generation of **[2a$^{\bullet}$]$^{+}$** from **2a** in this solvent at 253 K proceeds isosbestically, and leads to an increase in intensity for this peak, coupled to the ingrowth of a new shoulder near 23 × 10^3 cm^{-1} (Fig. 2). These changes strongly resemble those observed during the oxidation of mononuclear Pt(II)/cat/diphosphine complexes.[14] Importantly, the UV/vis/NIR spectrum of **[2a$^{\bullet}$]$^{+}$** shows no intervalence charge transfer (IVCT) absorption above 4000 cm^{-1}. That implies the electronic structure of **[2a$^{\bullet}$]$^{+}$** is class I valence-localised,[13] with no delocalisation or migration of the unpaired electron around the [tctq$^{\bullet}$]$^{5-}$ macrocycle. This contrasts with **[1a$^{\bullet}$]$^{+}$**, which shows an IVCT peak at ν_{max} = 7.9 × 10^3 cm^{-1} (ε_{max} = 500 M^{-1} cm^{-1}) indicating class II mixed-valent character.[14] Similar results were obtained from an oxidative titration of the **2a**/**[2a$^{\bullet}$]$^{+}$** couple with [Cp_2Fe]PF_6 at room temperature, although the transformation was not isosbestic under those conditions (ESI†).

No crystal structures of **2a** or **2b** were obtained during this study. However, comparison of metal-free H_6tctq·thf·*n*MeOH (*n* ≈ 0.15; ESI†) with published structures of H_6ctc shows small but consistent differences in the disposition of their dioxolene rings, which should also be reflected in their complexes.[12,14] The H_6tctq cavitand has a slightly shallower bowl-shaped conformation than H_6ctc (Fig. 3), which is reflected in the average intramolecular dihedral angle between the catechol rings in H_6tctq [62.9(1)°] and H_6ctc [typically 68–72°].[23,24] That might place the π-systems of the catechol rings in H_6tctq further apart. Conversely, the closest intramolecular contact between each catechol ring, namely the distance between their *ipso* C atoms at the base of the bowl-shaped cavity, is 2.513(4)–

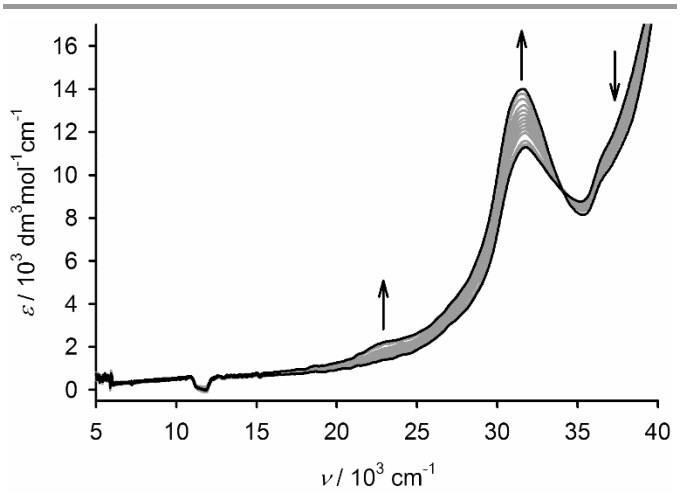

Fig. 2 The **2a**→**[2a•]**$^+$ oxidation at 253 K in CH_2Cl_2/0.1 M NBu_4PF_6, monitored by UV/vis/NIR spectroscopy using an optically transparent electrode. The spectra of the pure starting material and product are highlighted in black while the intermediate spectra are paler. The feature near 12 × 10^3 cm^{-1} is an artefact from a grating change in the spectrometer.

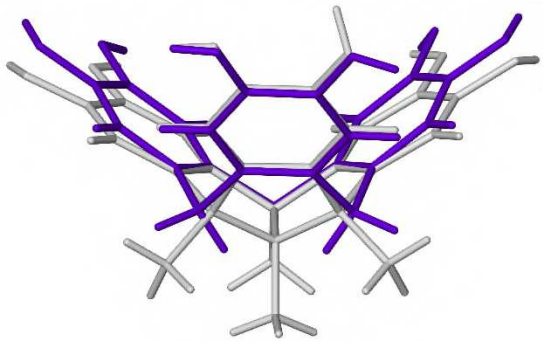

Fig. 3 Overlay of the crystallographic molecular structures of H_6tctq (white, ESI†) and H_6ctc (purple, from H_6ctc·5dmso[24]), showing the shallower bowl-shaped conformation of the H_6tctq macrocycle.

2.533(4) Å in H_6tctq which is similar to H_6ctc (typically 2.53–2.61 Å). Hence, there is no simple structural relationship between the dioxolene ligands in **[1a•]**$^+$ and **[2a•]**$^+$ that accounts for their different electronic character.

Geometry optimised structures and electronic properties of **[2a]**$^{0/1+/2+/3+}$ were calculated at the same level of theory used in our previous study of **[1a]**$^{0/1+/2+/3+}$.[14] That is, by spin-unrestricted broken symmetry DFT calculations at the B3LYP-ZORA level, with the dppb Ph groups replaced with H atoms. The optimized geometries of the [Pt(dppb)(dioxolene)] fragments in the two molecules show only small differences at each oxidation level (ESI†). The greatest differences lie in the Pt–P bonds which are consistently 0.012-0.019 Å longer in **[2a]**$^{z+}$ than in **[1a]**$^{z+}$ at each oxidation level *z*; and, the Pt–O bonds which are 0.014-0.019 Å shorter in **[2a•]**$^+$ than in **[1a•]**$^+$ (the Pt–O bond lengths in the two molecules are more similar for other *z*). This may reflect a stronger O→Pt σ-donation interaction in **[2a]**$^{z+}$, arising from the stronger inductive effect of its quaternary alkyl dioxolene substituents.

The average calculated Pt···Pt distances in **[2a]**$^{z+}$ and **[1a]**$^{z+}$ differ by no more than 0.012 Å at each oxidation level, and show the same trend of gradually increasing with *z*. Hence, in contrast to the free ligand crystallography (Fig. 3), the greater rigidity of the tctq macrocycle has little impact on the structures of its radical oxidation products at this level of theory. However, the ctc and tctq conformations will also be influenced by the inclusion of solvent molecules within their cavities, which is typically observed experimentally (ESI†) but is not accounted for in the geometry optimisation calculations.[14]

The calculated Mulliken spin density population (Figure 4) and UV/vis/NIR spectra of **[2a•]**$^+$ are essentially identical to **[1a•]**$^+$,[14] while the spin populations for the other members of the redox series are also identical irrespective of the ligand framework (ESI†). Since the DFT calculations are independent of temperature, that therefore suggests the different mixed-valent character of **[1a•]**$^+$ and **[2a•]**$^+$ arises from a temperature-dependent phenomenon. As the electronic structures are identical for both species, we attribute the spin-localisation in **[2a•]**$^+$ to the rigidity of the tctq ligand. The flexible secondary methylene groups in ctc can approach a π radial–σ-bond coplanar alignment with their bonded dioxolene groups, which would activate a through-bond interaction between the dioxolene π-systems *via* hyperconjugation.[25] This orientation is less accessible with the more rigid quaternary linkages in tctq, leading to localisation of the dioxolene spins as observed in **[2a•]**$^+$.

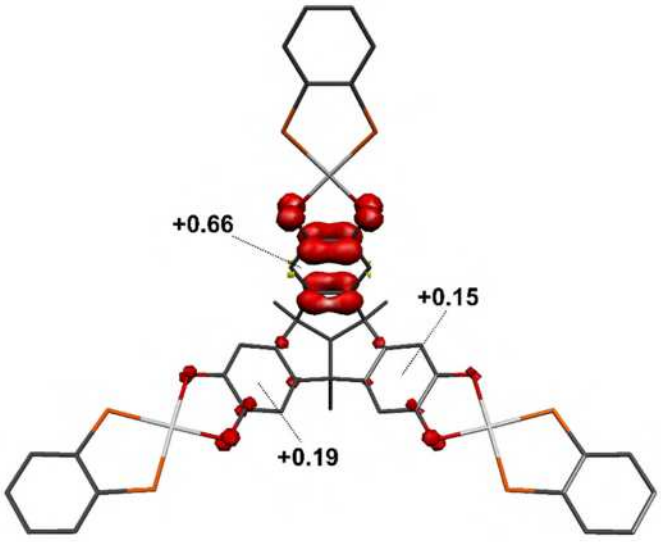

Fig. 4 Mulliken spin population analysis for **[2a•]**$^+$ (red: α-spin; yellow: β-spin).

In conclusion, we have demonstrated that the mixed-valent character of sq radicals derived from complexed cyclotricatechylene macrocycles is sensitive to their conformational flexibility. Our current work aims to make use of this feature in host:guest systems based on this redox-active molecular framework.

This work was funded by the EPSRC (EP/M506552/1) and a Leverhulme Trust Research Project Grant (RPG-2014-303, to NJP and KBV). Data supporting this study are available in the ESI† and at http://doi.org/10.5518/###.

Conflicts of interest

There are no conflicts to declare.

Notes and references

¶ A 2,3,6,7,10,11-hexahydroxytribenzotriquinacene *tris*-catechol related to H_6tctq, but lacking the methyl substituents on the macrocycle methylene groups, was recently reported.[26]

1 C. G. Pierpoint and C. W. Lange, *Prog. Inorg. Chem.*, 1993, **41**, 331; C. G. Pierpont and J. K. Kelly in *The Chemistry of Metal Phenolates Part [1, 2]*, ed. J. Zabicky, Wiley, Chichester, UK, 2014, pp. 669–698.

2 D. L. J. Broere, R. Plessius and J. I. van der Vlugt, *Chem. Soc. Rev.*, 2015, **44**, 6886 and 2015, **44**, 7010 and 7011 (corrections).

3 W. Kaim and B. Schwederski, *Coord. Chem. Rev.*, 2010, **254**, 1580; E. M. Shepard and D. M. Dooley, *Acc. Chem. Res.*, 2015, **48**, 1218.

4 J. Sedó , J. Saiz-Poseu , F. Busqué and D. Ruiz-Molina, *Adv. Mater.*, 2013, **25**, 653; J. Yang, M. A. Cohen Stuart and M. Kamperman, *Chem. Soc. Rev.*, 2014, **43**, 8271.

5 J. S. Miller and K. S. Min, *Angew. Chem. Int. Ed.*, 2009, **48**, 262; T. Tezgerevska, K. G. Alley and C. Boskovic, *Coord. Chem. Rev.*, 2014, **268**, 23.

6 J. A. DeGayner, I.-R. Jeon, L. Sun, M. Dincă and T. D. Harris, *J. Am. Chem. Soc.*, 2017, **139**, 4175; J. A. DeGayner, K. Wu and T. D. Harris, *J. Am. Chem. Soc.*, 2018, **140**, 6550; S. A. Sahadevan, A. Abhervé, N. Monni, C. Sáenz de Pipaón, J. R. Galán-Mascarós, J. C. Waerenborgh, B. J. C. Vieira, P. Auban-Senzier, S. Pillet, E. Bendeif, P. Alemany, E. Canadell, M. L. Mercuri and N. Avarvari, *J. Am. Chem. Soc.*, 2018, **140**, 12611.

7 J. Hankache and O. S. Wenger, *Chem. Rev.*, 2011, **111**, 5138; A. Heckmann and C. Lambert, *Angew. Chem., Int. Ed.*, 2012, **51**, 326.

8 C. G. Pierpont, *Inorg. Chem.*, 2011, **50**, 9766.

9 D. A. Shultz, *Comments Inorg. Chem.*, 2002, **23**, 1.

10 A. Dei, D. Gatteschi, C. Sangregorio and L. Sorace, *Acc. Chem. Res.*, 2004, **37**, 827.

11 K. G. Alley, G. Poneti, P. S. D. Robinson, A. Nafady, B. Moubaraki, J. B. Aitken, S. C. Drew, C. Ritchie, B. F. Abrahams, R. K. Hocking, K. S. Murray, A. M. Bond, H. H. Harris, L. Sorace and C. Boskovic, *J. Am. Chem. Soc.*, 2013, **135**, 8304.

12 D. S. Bohle and D. Stasko, *Chem. Commun*., 1998, 567.

13 K. D. Demadis, C. M. Hartshorn and T. J. Meyer, *Chem. Rev.*, 2001, **101**, 2655; D. M. D'Alessandro and F. R. Keene, *Chem. Soc. Rev.*, 2006, **35**, 424.

14 J. J. Loughrey, N. J. Patmore, A. Baldansuren, A. J. Fielding, E. J. L. McInnes, M. J. Hardie, S. Sproules and M. A. Halcrow, *Chem. Sci.*, 2015, **6**, 6935.

15 P. Chaudhuri and K. Wieghardt, *Prog. Inorg. Chem.*, 2001, **50**, 151.

16 D. Kuck, *Chem. Rev.*, 2006, **106**, 4885.

17 See *eg* J. Strübe, B. Neumann, H.-G. Stammler and D. Kuck, *Chem. Eur. J.*, 2009, **15**, 2256; T. Wang, Y.-F. Zhang, Q.-Q. Hou, W.-R. Xu, X.-P. Cao, H.-F. Chow and D. Kuck, *J. Org. Chem.*, 2013, **78**, 1062; W.-R. Xu, G.-J. Xia, H.-F. Chow, X.-P. Cao and D. Kuck, *Chem. Eur. J.*, 2015, **21**, 12011; Z.-M. Li, D. Hu, J. Wei, Q. Qi, X.-P. Cao, H.-F. Chow and D. Kuck, *Synthesis*, 2018, **50**, 1457.

18 B. Bredenkötter, S. Henne and D. Volkmer, *Chem. Eur. J.*, 2007, **13**, 9931; B. Bredenkötter, M. Grzywa, M. Alaghemandi, R. Schmid, W. Herrebout, P. Bultinck and D. Volkmer, *Chem. Eur. J.*, 2014, **20**, 9100.

19 J. Vile, M. Carta, C. G. Bezzu and N. B. McKeown, *Polym. Chem.*, 2011, **2**, 2257.

20 M. Harig, B. Neumann, H.-G. Stammler and D. Kuck, *Eur. J. Org. Chem.*, 2004, 2381.

21 J. A. Weinstein, M. T. Tierney, E. S. Davies, K. Base, A. A. Robeiro and M. W. Grinstaff, *Inorg. Chem.*, 2006, **45**, 4544; J. Best, I. V. Sazanovich, H. Adams, R. D. Bennett, E. S. Davies, A. J. H. M. Meijer, M. Towrie, S. A. Tikhomirov, O. V. Bouganov, M. D. Ward and J. A. Weinstein, *Inorg. Chem.*, 2010, **49**, 10041.

22 J. J. Loughrey, S. Sproules, E. J. L. McInnes, M. J. Hardie and M. A. Halcrow, *Chem. Eur. J.*, 2014, **20**, 6272.

23 J. A. Hyatt, E. N. Duesler, D.Y. Curtin and I. C. Paul, *J. Org. Chem.*, 1980, **45**, 5074; J. W. Steed, H. Zhang and J. L. Atwood, *Supramol. Chem.*, 1996, **7**, 37; A. Chakrabarti, H. M. Chawla, G. Hundal and N. Pant, *Tetrahedron*, 2005, **61**, 12323; P. Satha, G. Illa, P. Giriteja and S. Chandra, *Cryst. Growth Des.*, 2013, **13**, 2636.

24 J. J. Loughrey, C. A. Kilner, M. J. Hardie and M. A. Halcrow, *Supramol. Chem.*, 2012, **24**, 2.

25 K. Nunome, K. Toriyama and M. Iwasaki, *J. Chem. Phys.*, 1983, **79**, 2499; R. H. Contreras and J. E. Peralta, *Prog. Nucl. Magn. Reson.*, 2000, **37**, 321.

26 C.-F. Ng, H.-F. Chow, D. Kuck and T. C. W. Mak, *Cryst. Growth Des.*, 2017, **17**, 2822.